

## Supporting Information

### **DNAzyme-based lithium-selective imaging reveals higher lithium accumulation in bipolar disorder patient derived neurons**

Claire E. McGhee<sup>†,#</sup>, Zhenglin Yang<sup>‡,#</sup>, Weijie Guo<sup>‡,#</sup>, Yuting Wu<sup>†</sup>, Mingkuan Lyu<sup>†,||</sup>, Cynthia J. DeLong<sup>§</sup>, Shanni Hong<sup>†</sup>, Yuan Ma<sup>†</sup>, Melvin G. McInnis<sup>¶</sup>, K. Sue O'Shea<sup>§,¶</sup>, Yi Lu<sup>†,‡,||,\*</sup>.

†. Department of Chemistry, University of Illinois at Urbana-Champaign, Urbana, Illinois 61801, USA

‡. Department of Biochemistry, University of Illinois at Urbana-Champaign, Urbana, Illinois 61801, USA

||. Center for Advanced Bioenergy and Bioproducts Innovation, University of Illinois at Urbana-Champaign, Urbana, Illinois 61801, USA

§. Department of Cell and Developmental Biology, The University of Michigan, Ann Arbor, USA

¶. Department of Psychiatry, The University of Michigan, Ann Arbor, USA

#. These authors contributed equally to this work.

\*. Corresponding author. e-mail: yi-lu@illinois.edu

Contents	Page
Chemicals	S3
Table S1. DNA sequences for the in vitro selection and reselection of a Li <sup>+</sup> -DNAzyme.	S4
Table S2: The incubation time and concentration of LiCl for each round of selection.	S6
Table S3 Reselection incubation time for each round.	S7
Table S4 The measured $k_{obs}$ in response to different metal ions.	S8
Figure S1. The designed structure of N35 DNAzyme selection pool.	S9
Figure S2. The percentage of cleaved DNA after each round of selection.	S10
Figure S3. Sequence alignment of the 13 different sequences obtained from round 8.	S11
Figure S4. The activity and selectivity of round 8 sequences.	S12
Figure S5. A scheme showed the predicted secondary structure of the Original Li <sup>+</sup> DNAzyme by UNAFold calculation.	S13
Figure S6. The truncation study of the <i>cis-8-2</i> DNAzyme.	S14
Figure S7. A scheme showed the design of reselection pool.	S15
Figure S8. The percentage of cleaved DNA after each round of reselection.	S16
Figure S9. The aligned sequences from reselection.	S17
Figure S10. A scheme showed the 20-4 DNAzyme and the original DNAzyme.	S18
Figure S11. The activity of the 20-4 DNAzyme and the original DNAzyme.	S19
Figure S12. Optimization of binding arm sequences.	S20
Figure S13. Fluorescence increases of the active sensor over time at different Li <sup>+</sup> concentrations in the MOPS selection buffer.	S21
Figure S14. Linear detection range of the Li <sup>+</sup> DNAzyme sensor at the 6-hour time point in MOPS selection buffer.	S22
Figure S15. Fluorescence response of the inactive sensor over time at different Li <sup>+</sup> concentrations in the MOPS selection buffer.	S23
Figure S16. Li <sup>+</sup> toxicity to HeLa cell with 12 hours incubation.	S24
Figure S17. Li <sup>+</sup> imaging in PC12 and PC12-differentiated neurons.	S25
Figure S18. Quantification of fluorescence intensity from PC12 and PC12-differentiated neurons.	S26
Figure S19. Inactive DNAzyme imaging in human NPCs.	S27
Figure S20. Quantification of fluorescence intensity from NPCs.	S28
Figure S21. Inactive DNAzyme imaging in iPSCs-derived neurons.	S29
Figure S22. Quantification of fluorescence intensity from iPSCs-derived neurons.	S30
Figure S23. Intracellular Li <sup>+</sup> imaging in NPCs and neurons under 3mM Li <sup>+</sup> treatment.	S31
Figure S24. Positive transfection (control DNAzyme with fluorophores but without quenchers) in neurons with TurboFect.	S32
Figure S25. ICP detection of lithium and sodium total content in NPCs.	S33

## Chemicals

Acrylamide/bisacrylamide 40 % solution (29:1) was obtained from Bio-Rad Laboratories, Inc. The following enzymes, reaction buffers, and reagents used were purchased from New England Biolabs: Taq polymerase, standard Taq buffer, T4-polynucleotide kinase, polynucleotide kinase buffer, and deoxynucleotide (dNTP) solution mix. Both  $^{32}\text{P}$  labeled  $\alpha$ -ATP and  $\gamma$ -ATP were obtained from Perkin-Elmer. All PCR and  $^{32}\text{P}$ -labeling experiments were carried out in the BioRad thermocycler.

The following chemicals were as obtained as follows: 3-(N-morpholino)propanesulfonic acid (MOPS) (Amersham International plc), Urea (Affymetrix, MB grade), Tris (Affymetrix, MB grade), boric acid (Fischer Scientific, electrophoresis grade), Ethylenediaminetetraacetic acid (EDTA) (Fluka, 99.0%), EDTA·2Na·2H<sub>2</sub>O (Fisher Scientific), 200 proof ethanol (Decon Laboratories, Inc.), sodium acetate, , HCl (Alfa-Aesar, ultrapure), lithium hydroxide (Alfa aesar 99.999% puratonic salts), potassium hydroxide, sodium hydroxide, HCl (Alfa-Aesar, ultrapure). All of the metal salts used were obtained as listed: LiCl (Alfa aesar 99.999% puratonic salts), NaCl (Alfa aesar 99.999% puratonic salts), KCl (Alfa aesar 99.999% puratonic salts), CsCl (Alfa aesar 99.999% puratonic salts), RbCl (Alfa aesar 99.999% puratonic salts), MgCl<sub>2</sub> (Alfa aesar 99.999% puratonic salts), CaCl<sub>2</sub> (Alfa aesar 99.999% puratonic salts), PbCl<sub>2</sub> (Alfa aesar 99.999% puratonic salts), MnCl<sub>2</sub>(Alfa aesar 99.999% puratonic salts), SrCl<sub>2</sub> (Alfa aesar 99.999% puratonic salts), CoCl<sub>2</sub> (Alfa aesar 99.999% puratonic salts), BaCl<sub>2</sub> (Alfa aesar 99.999% puratonic salts), ZnCl<sub>2</sub> (Alfa aesar 99.999% puratonic salts), HgCl<sub>2</sub> (Alfa aesar 99.999% puratonic salts). All prepared metal ion, buffer, and gel, and desalting solutions used Milli-Q water with no additional treatment. The pH of relevant solutions was confirmed using the Fisher Scientific Accumet AB15 pH meter.

## Supplemental Tables.

Table S1. DNA sequences ordered for the in vitro selection and reselection of a Li<sup>+</sup>-DNAzyme.

Name	Sequence (5' to 3')
P2	GEATCTTACTTCAGTTAGGGAGACTCGCACG
P3-Opt	GATACATAGCATCTTACTTCAGTTAG
P3-rG	GATACATAGCATCTTACTTCAGTTArG
P1-iSp18	GACAACAACAACAAC-iSp18-GACCGGACCTCCTTCAG
P1	GACCGGACCTCCTTCAG
IDT Template (N35)	GACAACAACAACAAC-iSp18-GACCGGACCTCCTTCAG-cN35- GACTCATGCGAGTCTCCCTAACTGAAGTAAGATGCTATGTATC
IDT Pool (N25)	GATACATAGCATCTTACTTCAGTTArGGGAGACTCGCACGAGTC-N25- CTGAAGGAGGTCCGGTC
fP-LiR18	GACAACAACAACAAC-iSp18-GACGTGAAGTTCTACAG
rP-LiR18	ATCTCACTACAGTTAGGGAGTCACGCTAG
rP-LiR18-rG	CTATCCATCTCACTACAGTTArG
Template (N18)	CCATCTCACTACAGTTArGGGAGTCACGCTAGTGACtcgataagcaaccgataaCT GTAGAACTTCACGTC
Original DNAzyme	GATACATAGCATCTTACTTCAGTTArGGGAGACTCGCACGAGTCTCGATA AGCAACCGATAACTCAATAGATGCCCCCTGAAGGAGGTCCGGTC
cis 20-4	CTATCCATCTACTACAGTTArGGGAGTCACGCTAGGGACTCGATCAGCAA CCGAGAACTGTAGAACTTCACGTC
trans 20-4 aE	GTACGAGAGT CGATCAGCAACCGAG AACTGTAGTGG
trans 20-4 iE	GTACGAGAGT CCTAGTCGTTGGCTC AACTGTAGTGG
trans 20-4 rS	CCACTACAGTTArGGGACTCTCGTAC
trans-rS 11- 10 uni arm	CACTCACTATTArGGGAGGAAGAGAT
trans-aE 11- 10 uni arm	ATCTCTTCCTC GATCAGCAACCGAG AATAGTGAGTG
trans-rS 9-9 sel arm	CCACTCGTTArGGGACCCGTTAC
trans-aE 9-9 sel arm	GTAACGGGTC GATCAGCAACCGAG AACGAGTGG
trans-rS 13- 13 sel arm	CTCCACTACAGTTArGGGACTCTCGTACTCC
trans-aE 13- 13 sel arm	GGAGTACGAGAGTC GATCAGCAACCGAG AACTGTAGTGGAG
20-4 rS A488	/5Alex488N/CACTCACTATTArGGGAGGAAGAGAT/3IABkFQ/

20-4 aE ATCTCTTCCTC GATCAGCAACCGAG AATAGTGAGTG/3IABkFQ/  
IABFQ  
20-4 iE ATCTCTTCCTC CTAGTCGTTGGCTC AATAGTGAGTG/3IABkFQ/  
IABFQ

---

\*Lower case a indicates 70% dA, 10% each dG, dC, and dT wobble site

\*Lower case g indicates 70% dG, 10% each dA, dC, and dT wobble site

\*Lower case c indicates 70% dC, 10% each dG, dA, and dT wobble site

\*Lower case t indicates 70% dT, 10% each dG, dC, and dA wobble site

Table S2: The incubation time of the N35 pool with the indicated concentration of LiCl for each round of selection

Selection Round	Incubation Time (h)	[Li+] (mM)
1-7	2	200
8	1.5	200
9	1.08	200
10	0.5	200

Table S3 Reselection incubation time for each round.

Selection Round	Incubation Time (min)	[Li <sup>+</sup> ] (mM)
1	180	70
2	120	70
3	90	70
4	60	70
5	30	70
6	15	70
7	10	70
8	8	70
9	6	70
10	5	70
11-15	4	70
16	2.5	70
17	2	70
18	1.5	70
19-20	1	70

Table S4 The measured  $k_{\text{obs}}$  in response to different metal ions

Metal ion	Concentration (mM)	$k_{\text{obs}}$ ( $\text{h}^{-1}$ )	Fold selectivity compared with the 200 mM $\text{Li}^+$ group
$\text{Li}^+$	200	0.221	
$\text{Na}^+$	200	1.55 E-3	143
$\text{K}^+$	200	9.14 E-4	242
$\text{Rb}^+$	200	9.05 E-4	244
$\text{Cs}^+$	200	7.11 E-4	311
$\text{NH}_4^+$	200	5.02 E-3	44
$\text{Mg}^{2+}$	4	2.12 E-3	104
$\text{Ca}^{2+}$	4	9.26 E-6	23866
$\text{Sr}^{2+}$	4	9.29 E-4	238
$\text{Ba}^{2+}$	4	7.13 E-4	310
$\text{Co}^{2+}$	4	1.78 E-3	124
$\text{Mn}^{2+}$	4	1.14 E-2	19
$\text{Hg}^{2+}$	4	1.93 E-5	11451
$\text{Pb}^{2+}$	4	3.10 E-4	713
$\text{Fe}^{3+}$	0.4	9.25 E-4	239
$\text{In}^{3+}$	0.4	1.18 E-3	187



Supplemental Figures.

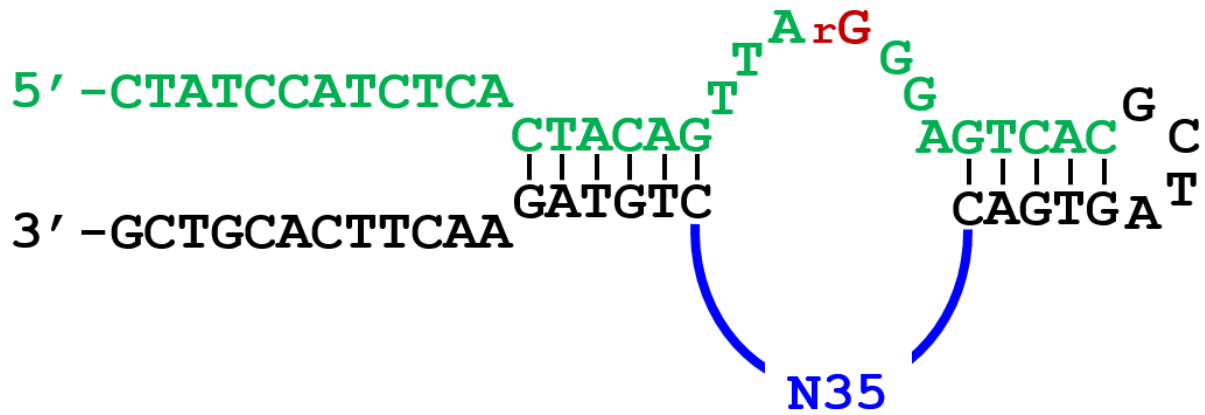


Figure S1. The designed structure of N35 DNAzyme selection pool. The conserved sequences flanking N35 random region are shown. Ribonucleotide cleaving site is shown in red. Designed substrate arm and random region inside the enzyme arm are shown in green and blue.

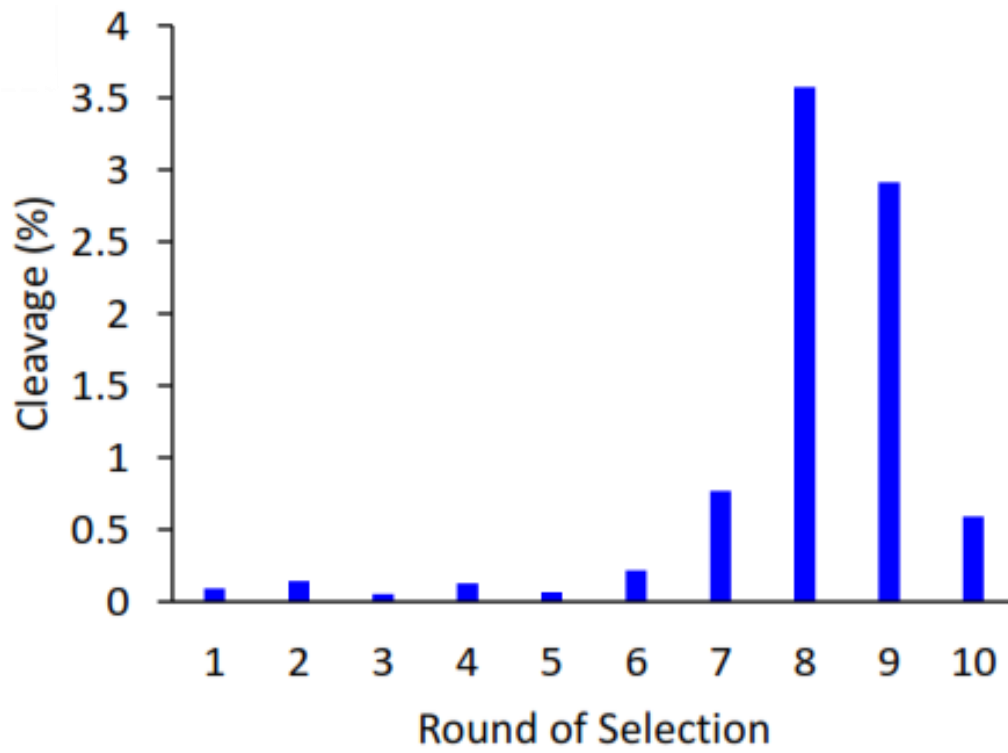


Figure S2. The percentage of cleaved DNA after each round of selection for the N35 pool.

```

2, 5, 8, 17, 36, 54, 55, 71, 79, 86, 88, 90 GATACATAGCA TCTTACTTCAGTTAGGGAGACTCGCACGAGTC TCGATAAGCAACCGATAACTCAATAGATGCCCCCCCT -GAAGGAGGTCCGGTC
30, 35 --GAACAAGCA TCTTACTTCAGTTAGGGAGACTCGCACGAGTC TCGATAAGCAACCGATAACTCAATAGACGCCCCCCCT -GAAGGAGGTCCGGTC
99 GATACATAGCA TCTTACTTCAGTTAGGGAGACTCGCACGAGTC TCGATAAGCGACCGATAACTCGATAGGTGCCCCCCCT -GAAGGGGTCCGGTC-
4 GATACATAGCA TCTTACTTCAGTTAGGGAGACTCGCACGAGTC TCGATAAGCAACCGATAACTCAATAGATGCCCGCCCTG -AAGGAGGTCCG-GTC
73, 76 GATACATAGCA TCTTACTTCAGTTAGGGAGACTCGCACGAGTC CGTAGCATAGTGTTACAACGTGTGGCTCCCCCGTCCCT GAAGGAGGTCCG-GTC
94 GATACATAGCA TCTTACTTCAGTTAGGGAGACTCGCACGAGTC GGTAGCCGTCCATCCTCCCTTTCCACCCCGTGTGCCT GAGGGGGTCCG-TTC
42 GATACATAGCA TCTTACTTCAGTTAGGGAGACTCGCACGAGTC CATGTAACATGTTTCCAAGAATACGTTCCCGCCCT GAAGGAGGTCCG-GTC
67 GATACATAGCA TCTTACTTCAGTTAGGGAGACTCGCACGAGTC GCCTGATAGGCAGTATATCGATAACACTATGCTACCT GAAGGAGGTCCG-GTC
12 GATACATAGCA TCTTACTTCAGTTAGGGAGACTCGCACGAGTC GACTTAAATCCCGATCCTGAGCAGCCTTCCCGCCT GAAGGAGGTCCG-GTC
82 GATACATAGCA TCTTACTTCAGTTAGGGAGACTCGCACGAGTC GTTATGTCCGCGCTCGACAGTACGTATGTGTGGTCCCT GAAGGAGGTCCG-GTC
14 GATACATAGCA TCTTACTTCAGTTAGGGAGACTCGCACGAGTC ACTATAGTCACTAGAGTTTATCTTACGTGGTGCCT GAAGGAGGTCCG-GTC
26 GATACATAGCA TCTTACTTCAGTTAGGGAGACTCGCACGAGTC GACTGCCGTGATTGGATAATCCACCCTCCCTCCCCCT GAAGGAGGTCCGGTC
43 GATACATAGCA TCTTACTTCAGTTAGGGAGACTCGCACGAGTC CCGGAGAGATGCATATACGAACCTCCACTTCC-----
* * * * *

```

Figure S3. Sequence alignment of the 13 different sequences obtained from round 8. The programmed sequences are highlighted in red and green, with the random region shown in between. Sequences with highly homologous regions are highlighted in blue with single based mutations between these sequences indicated in red letter. The numbers to the left of the sequence indicate the name of the sequence upon submission to sequences.

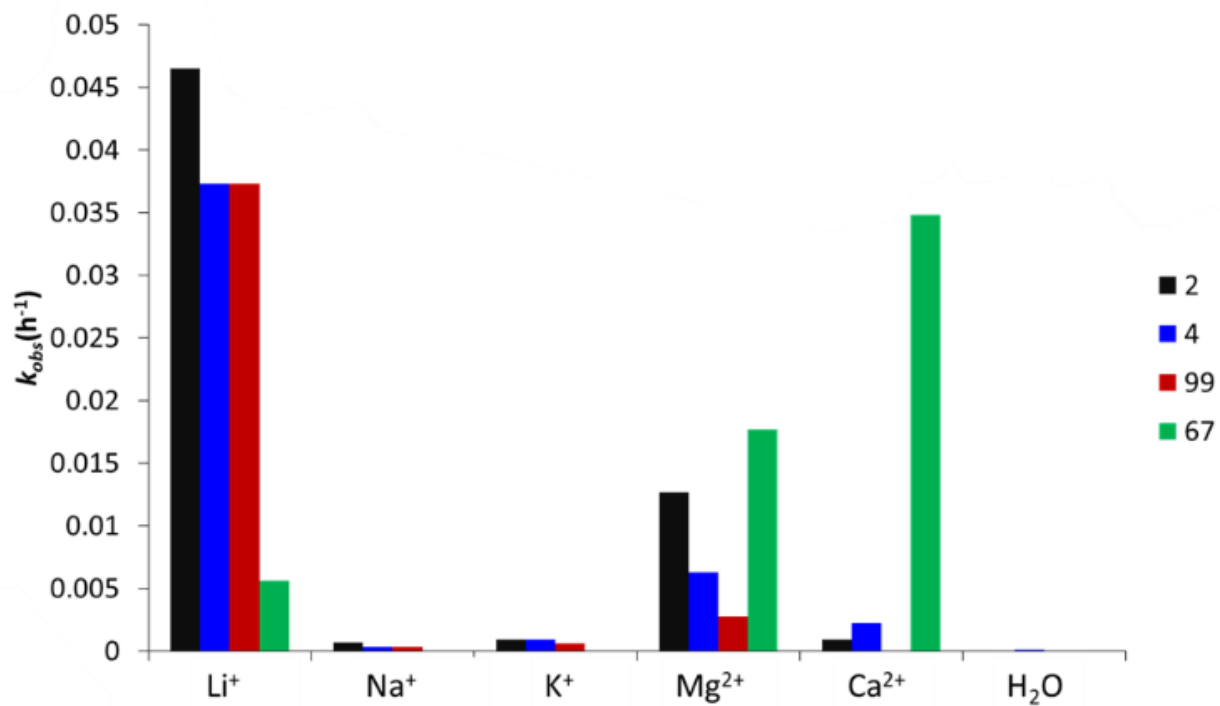


Figure S4. The activity and selectivity of round 8 sequences in 200 mM  $M^+$  or 10 mM  $M^{2+}$  in 20 mM MOPS pH 7.4

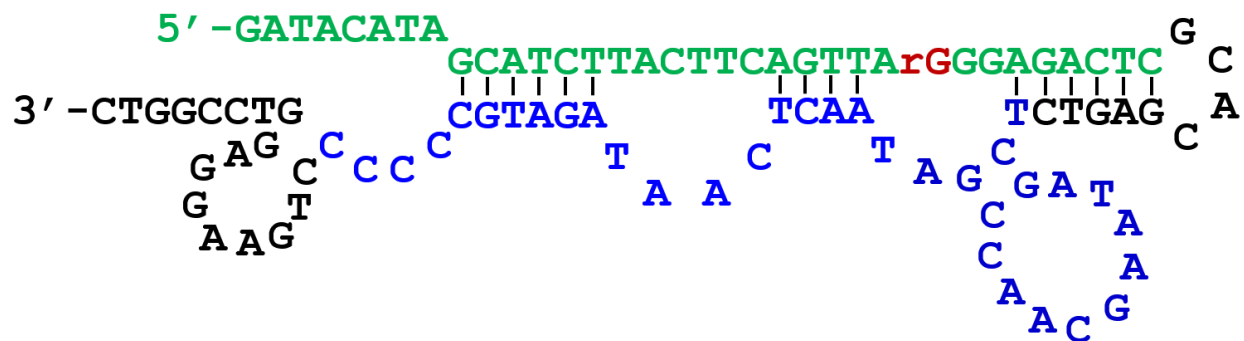


Figure S5. A scheme showed the predicted secondary structure of the Original Li<sup>+</sup> DNzyme by UNAFold calculation, where the random region is shown in blue, the active site in red, and the designed substrate arm in green.

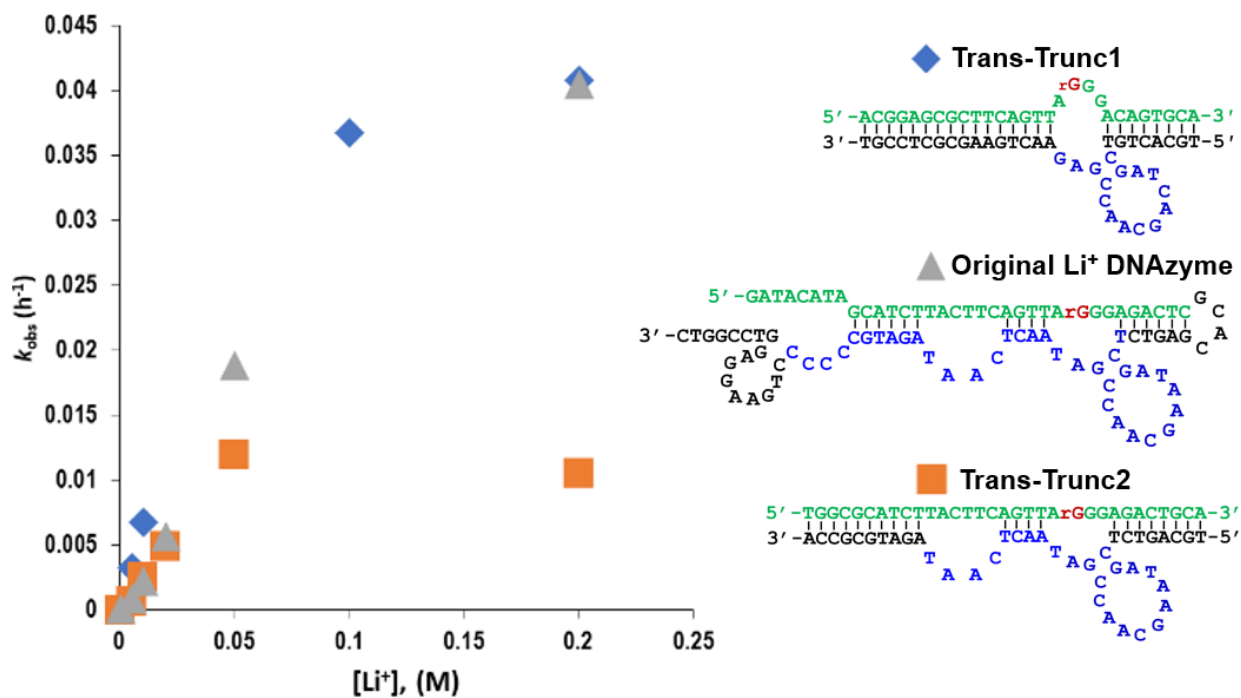
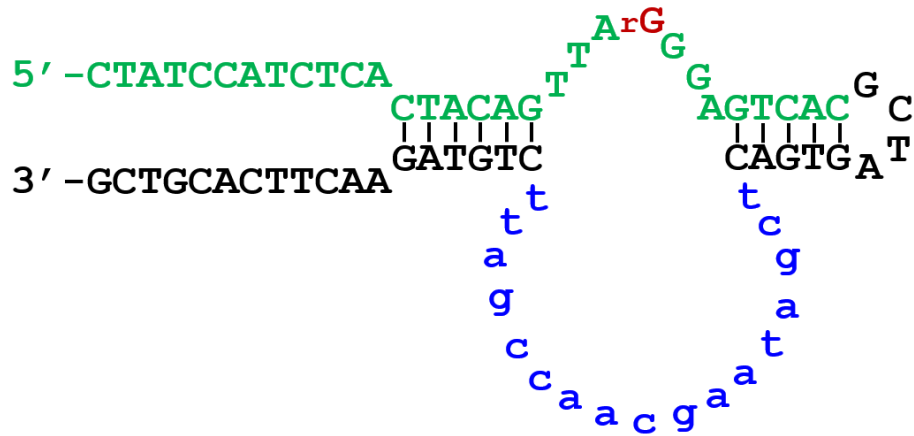


Figure S6. The truncation study of the *cis-8-2* DNAzyme. The predicted secondary structures and activity traces are shown for different truncations. The *trans-Trunc1* variance showed comparable activity to the original  $\text{Li}^+$  DNAzyme.



- \*Lower case a indicates 70% dA, 10% each dG, dC, and dT wobble site
- \*Lower case g indicates 70% dG, 10% each dA, dC, and dT wobble site
- \*Lower case c indicates 70% dC, 10% each dG, dA, and dT wobble site
- \*Lower case t indicates 70% dT, 10% each dG, dC, and dA wobble site

Figure S7. Scheme showed the design of reselection pool. Blue nucleotides indicate partially randomized region, which is 18 nucleobases long (15 nt catalytic loop + 3 nt flanking sites) and based on a 30 % mutation rate (70% of the original nucleotide and 10% of the nucleotide other than the original nucleotide each) of the *trans-Trunc1* enzyme sequence.

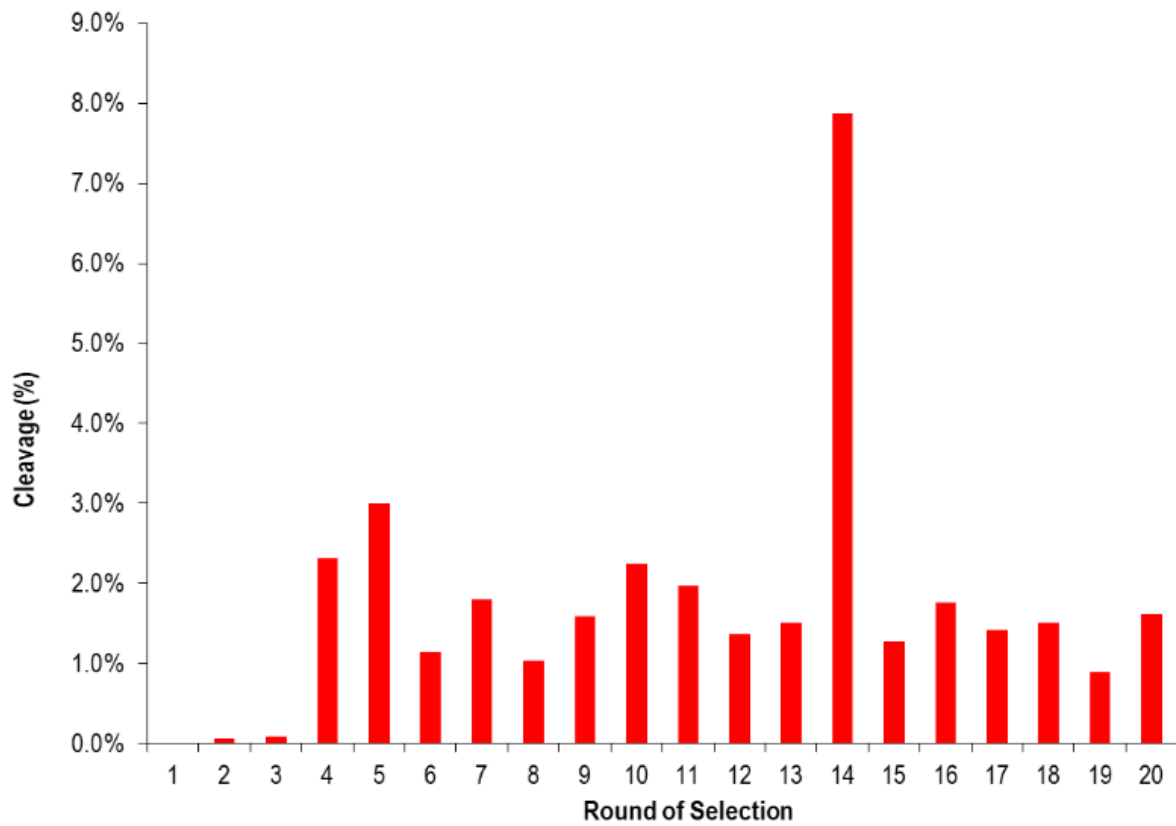


Figure S8. The percentage of cleaved DNA from the reselection pool after each round of selection. Round 20 pool showed the significant activity even with reaction time as short as 1 min.



OR: CTATCCATCTCACTACAGTTArGGGAGTCACGCTAGTGAC-TCGATAAGCAACCGATAA-CTGTAGAACTTCACGTC  
 04: CTATCCATCTCACTACAGTTArGGGAGTCACGCTAGGGAC-TCGATCAGCAACCGAGAA-CTGTAGAACTTCACGTC high  
 27: CTATCCATCTCACTACAGTTArGGGAGTCACGCTAGTGAG-TCGATTAGCAACCGAGAA-CTGTAGAACTTCACGTC med  
 50: CTATCCATCTCACTACAGTTArGGGAGTCACGGCTAGGGACTCGATAAGCAACCGAGAA-CTGTAGAACTTCACGTC med-high  
 54: CTATCCATCTCACTACAGTTArGGGAGTCACGCTAGGGAC-TCGATCAGCAACCGATAA-CTGTAGAACTTCACGTC med-high  
 58: CTATCCATCTCACTACAGTTArGGGAGTCACGCTAGTGCC-TCGATAAGCAACCGATAA-CTGTAGAACTTCACGTC med-low  
 60: CTATCCATCTCACTACAGTTArGGGAGTCACGCTAGTGAG-TCGATCAGCAACCGATAG-CTGTAGAACTTCACGTC low  
 11: CTATCCATCTCACTACAGTTArGGGAGTCACGCTAGGGAC-TCGATCACAACCGAGAA-CTGTAGAACTTCACGTC no act  
 21: CTATCCATCTCA-TACAGTTArGGGAGTCACGCTAGGGAC-TCGATCCGCAACCGAGAA-CTGTAGAACTTCACGTC no act

Figure S9. The aligned sequences from selection are shown with “OR” indicating the original sequence. The sequence name is shown on the left, and the relative activity is indicated on the right. Sequences with med-low activity are highlighted in yellow, low activity in orange, and no activity in red.

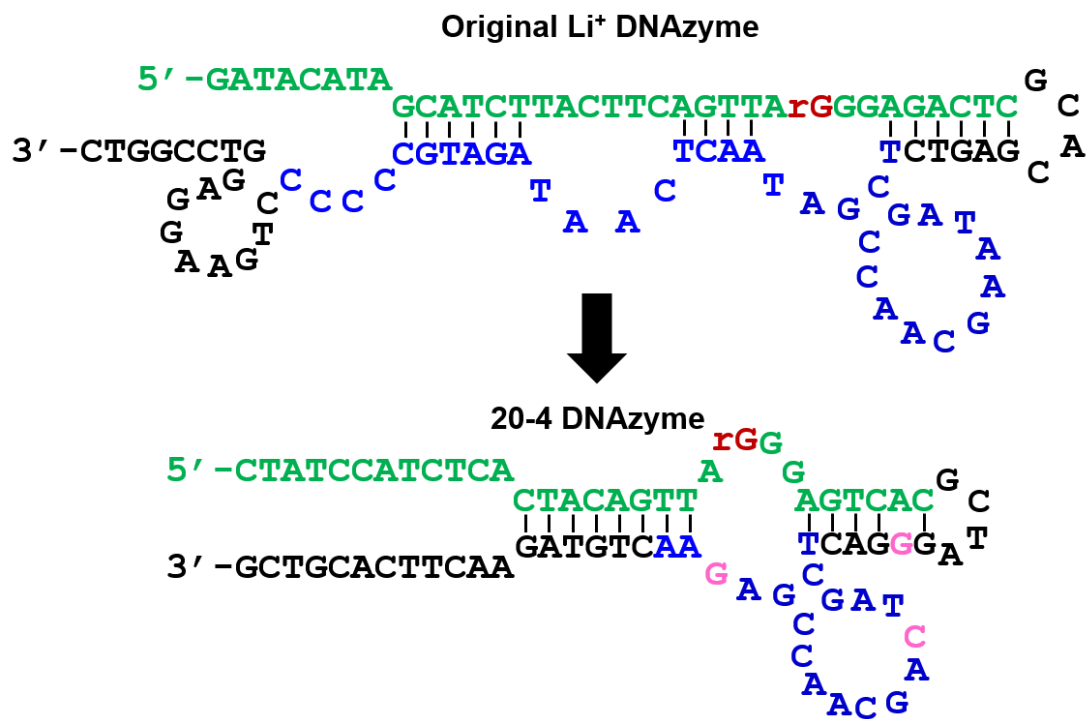


Figure S10. Schematic representation of the newly selected 20-4 DNAzyme compared with the original DNAzyme it is based upon, with point mutations highlighted in pink.

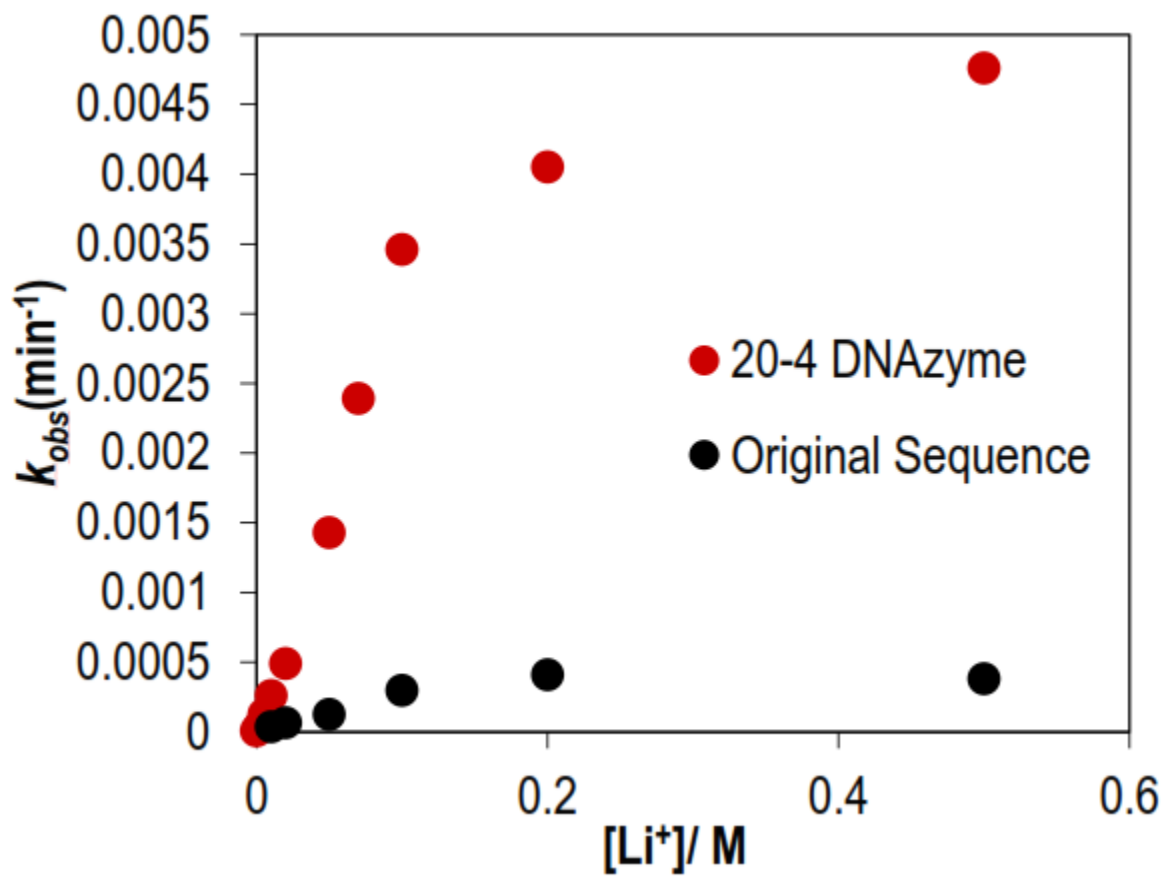


Figure S11. A comparison of the activity of the 20-4 DNAzyme selected from partial randomization, and the previously selected DNAzyme the selection is based on at varying lithium concentrations.

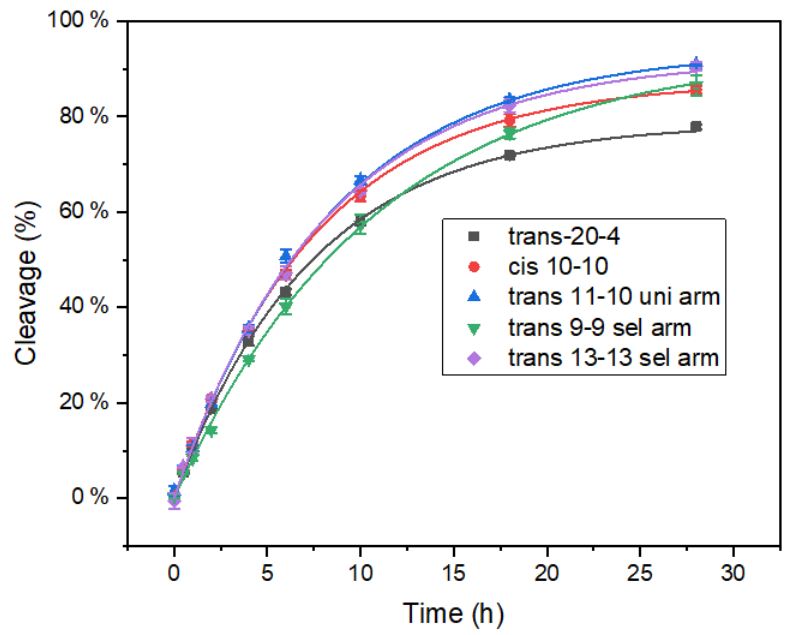


Figure S12. Optimization of binding arm sequences to achieve successful dehybridization of the cleaved substrate strands.

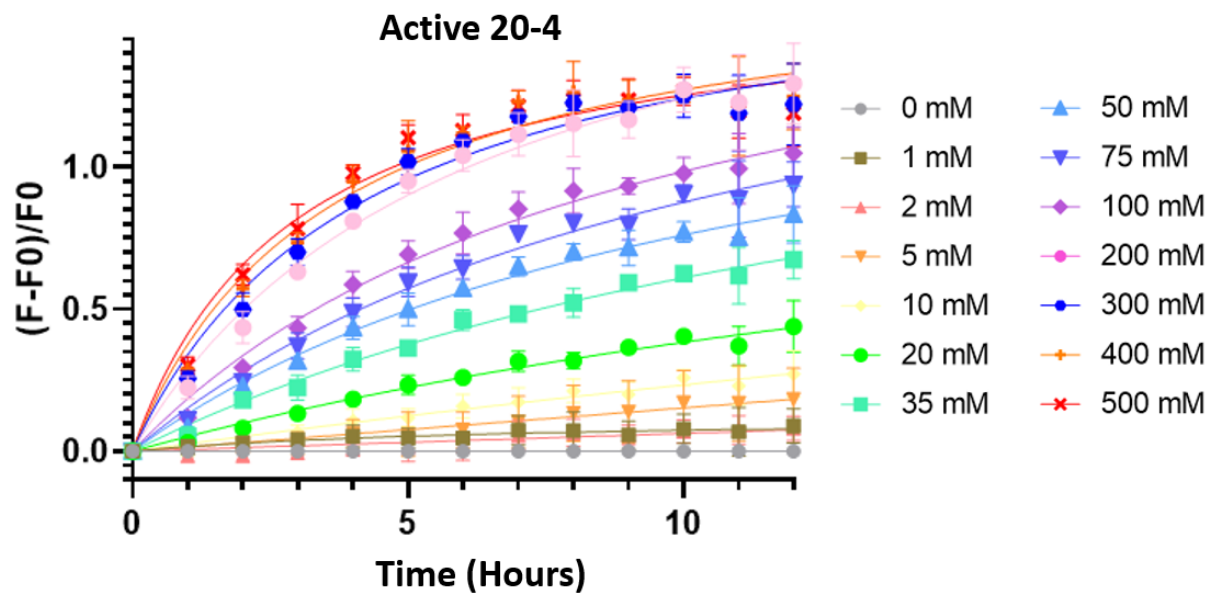


Figure S13. Fluorescence increases of the active sensor over time at different  $\text{Li}^+$  concentrations in the MOPS selection buffer. Plots show Mean  $\pm$  S.D.  $n=3$  for each group.

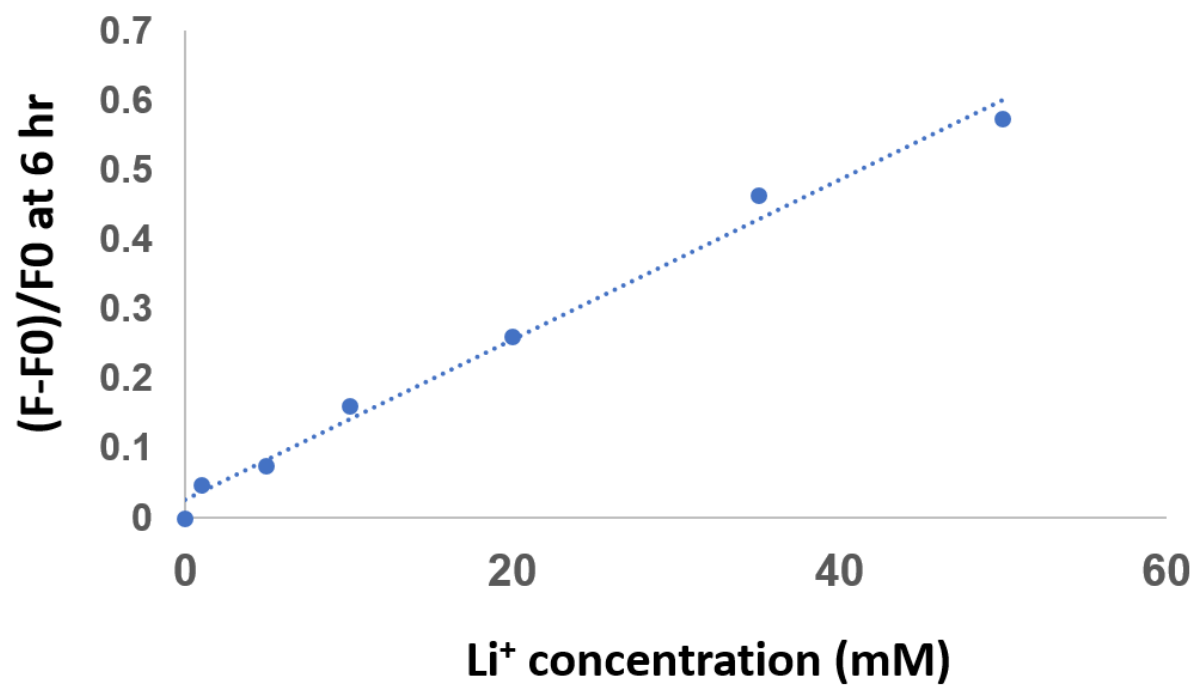


Figure S14. Linear detection range of the  $\text{Li}^+$  DNzyme sensor at the 6-hour time point in MOPS selection buffer.

### Inactive 20-4

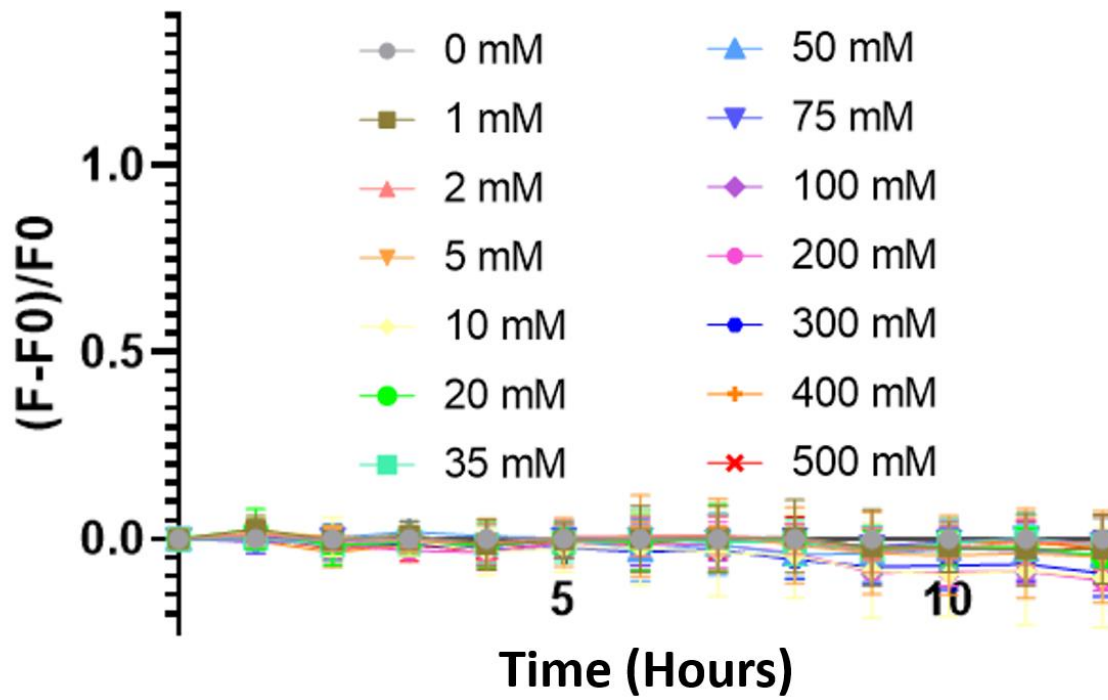


Figure S15. Fluorescence response of the inactive sensor over time at different Li<sup>+</sup> concentrations in the MOPS selection buffer. Plots show Mean +/- S.D. n=3 for each group.

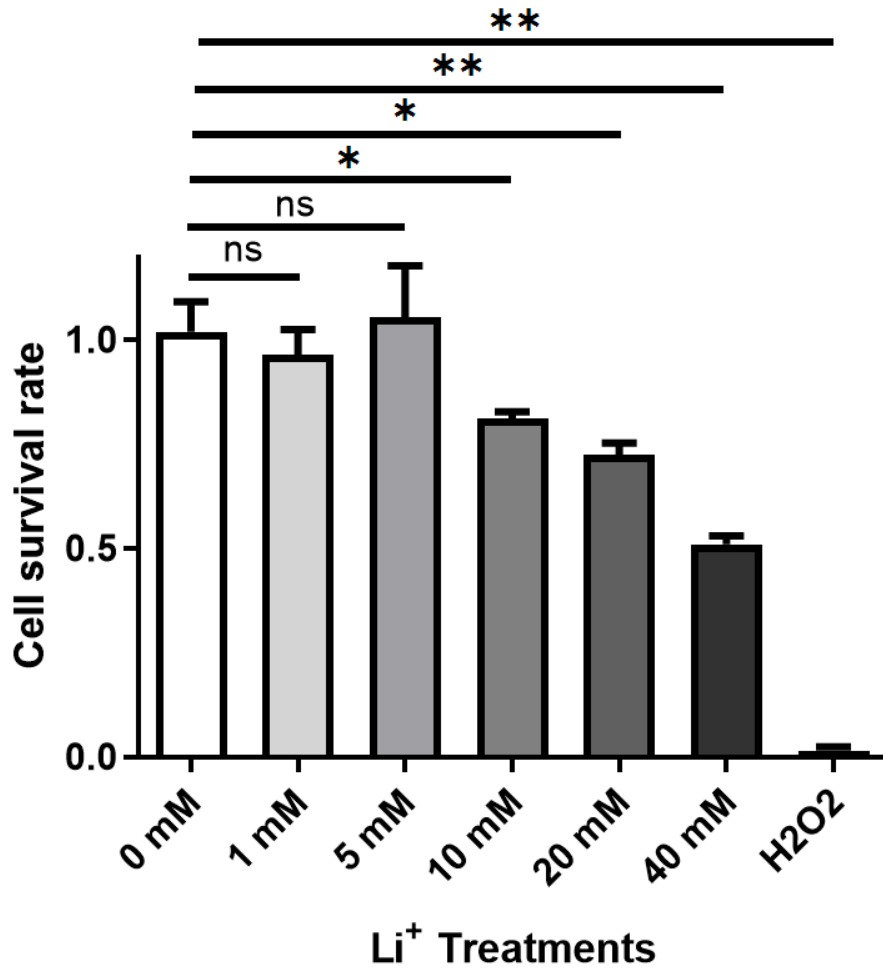


Figure S16. Li<sup>+</sup> toxicity to HeLa cell with 12 hours incubation. Data shown in mean and S.D. n=3 for each group. Two tailed paired t-test; ns p=0.5476>0.05 between 0 mM and 1 mM groups, ns p=0.6153>0.05 between 0 mM and 5 mM groups, \* p=0.0230<0.05 between 0 mM and 10 mM groups, \* p=0.0285<0.05 between 0 mM and 20 mM groups, \*\* p=0.0057<0.01 between 0 mM and 40 mM groups, \*\* p=0.0015<0.01 between 0 mM and H<sub>2</sub>O<sub>2</sub> groups.



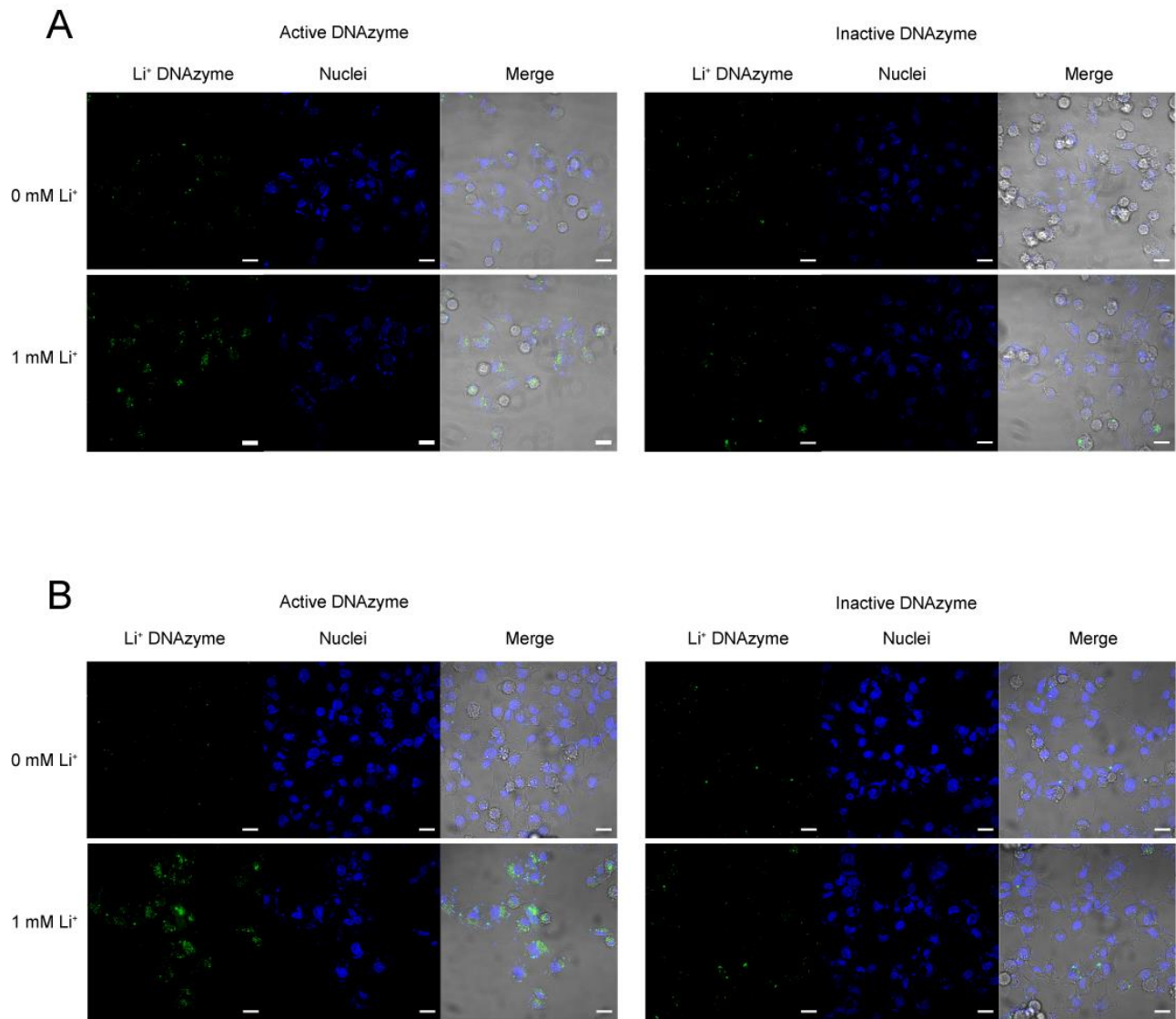


Figure S17. Li<sup>+</sup> imaging in PC12 (A) and PC12-differentiated neurons (B) with active (left) or inactive (right) 20-4 sensors. Scale bar: 20  $\mu$ m

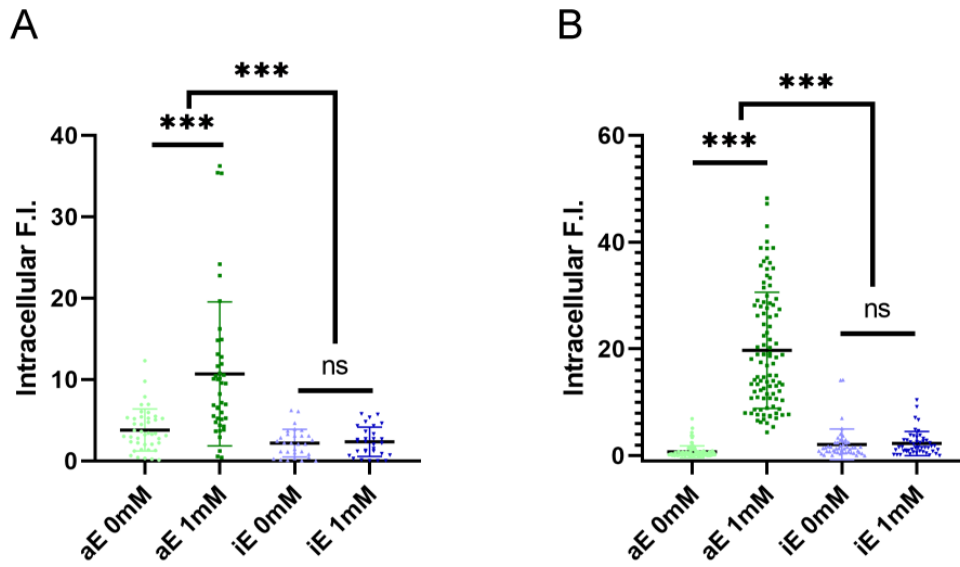


Figure S18. Plot graph shows the quantification of fluorescence intensity from PC12 (A) and PC12-differentiated neurons (B). Data shown in mean and S.D. Mann-Whitney test; ns  $p > 0.05$ ; \*\*\*  $p < 0.001$ .

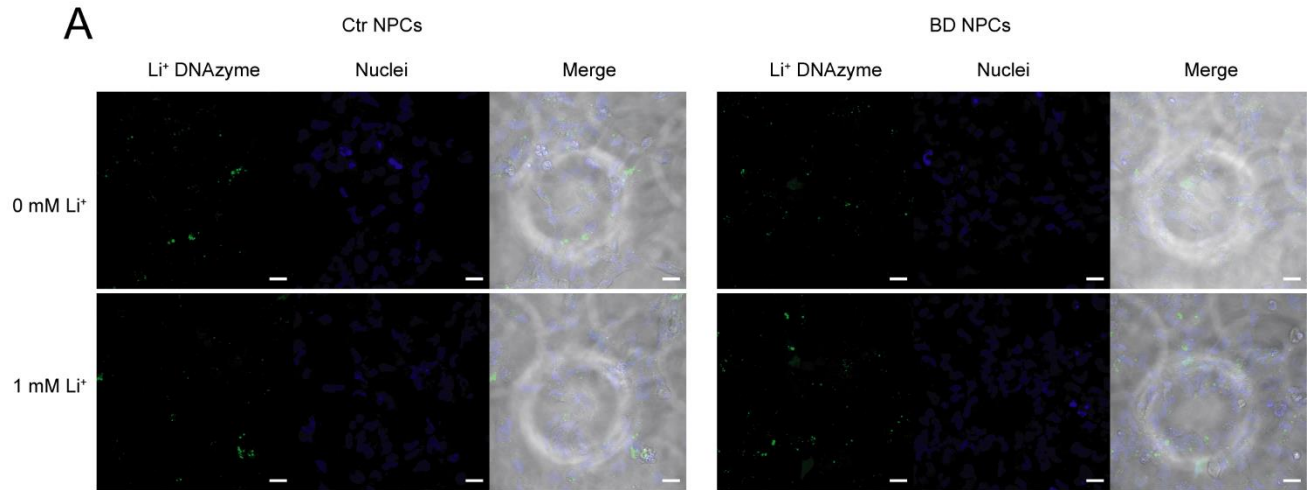


Figure S19. Inactive DNAzyme imaging in human neural progenitor cells (NPCs) from bipolar disorder patient and healthy donor. Scale bar: 20  $\mu$ m

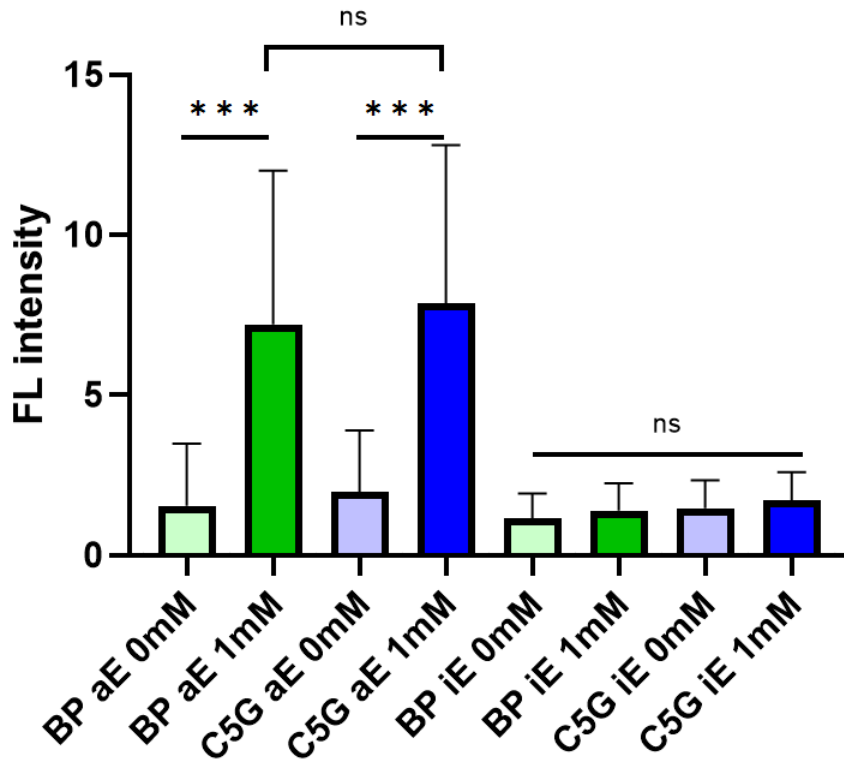


Figure S20. Bar graph shows the quantification of fluorescence intensity from NPCs derived from BD patients and healthy controls. Data shown in mean and S.D. Two-tailed unpaired t-test; ns  $p > 0.05$ ; \*\*\*  $p < 0.001$ .

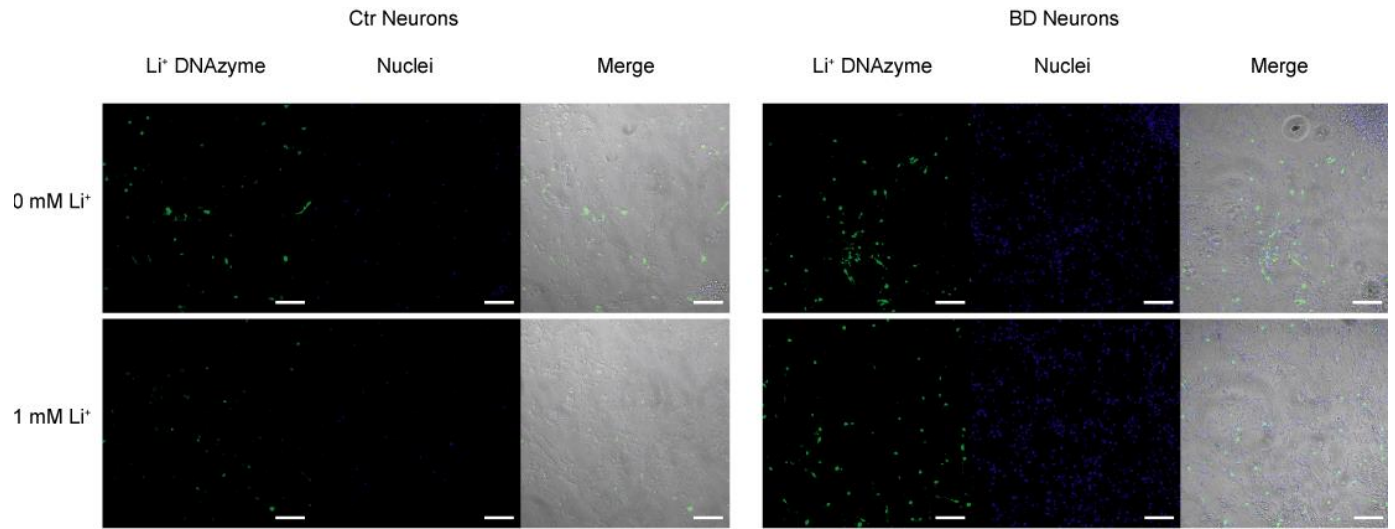


Figure S21. Inactive DNAzyme imaging in iPSCs-derived neurons from bipolar disorder patient (right) and healthy donor (left). Scale bar: 100  $\mu$ m

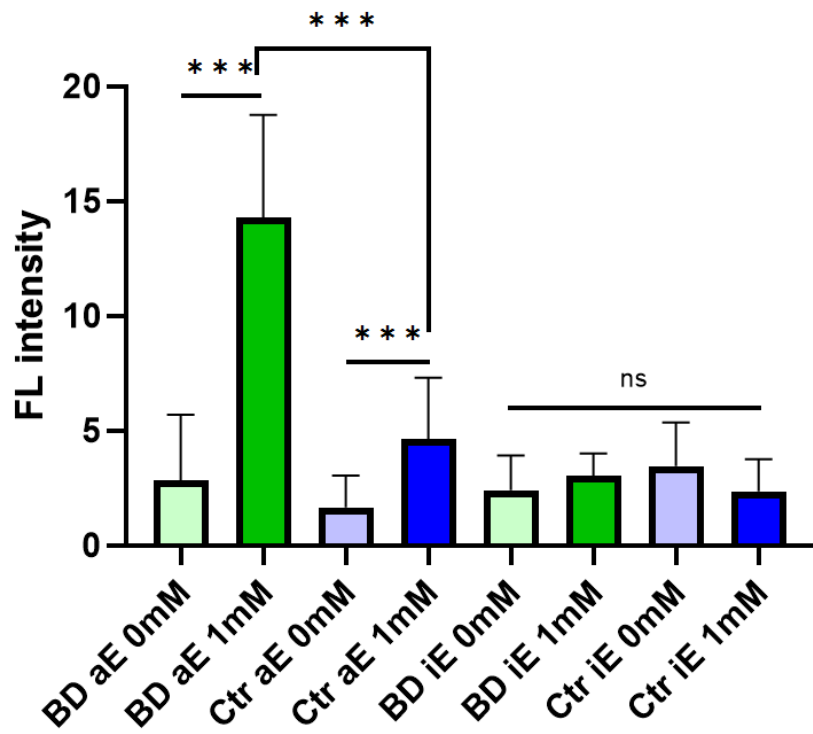


Figure S22. Bar graph shows the quantification of fluorescence intensity from neurons derived from BD patients and healthy controls. Data shown in mean and S.D. Two-tailed unpaired t-test; ns  $p > 0.05$ ; \*\*\*  $p < 0.001$ .

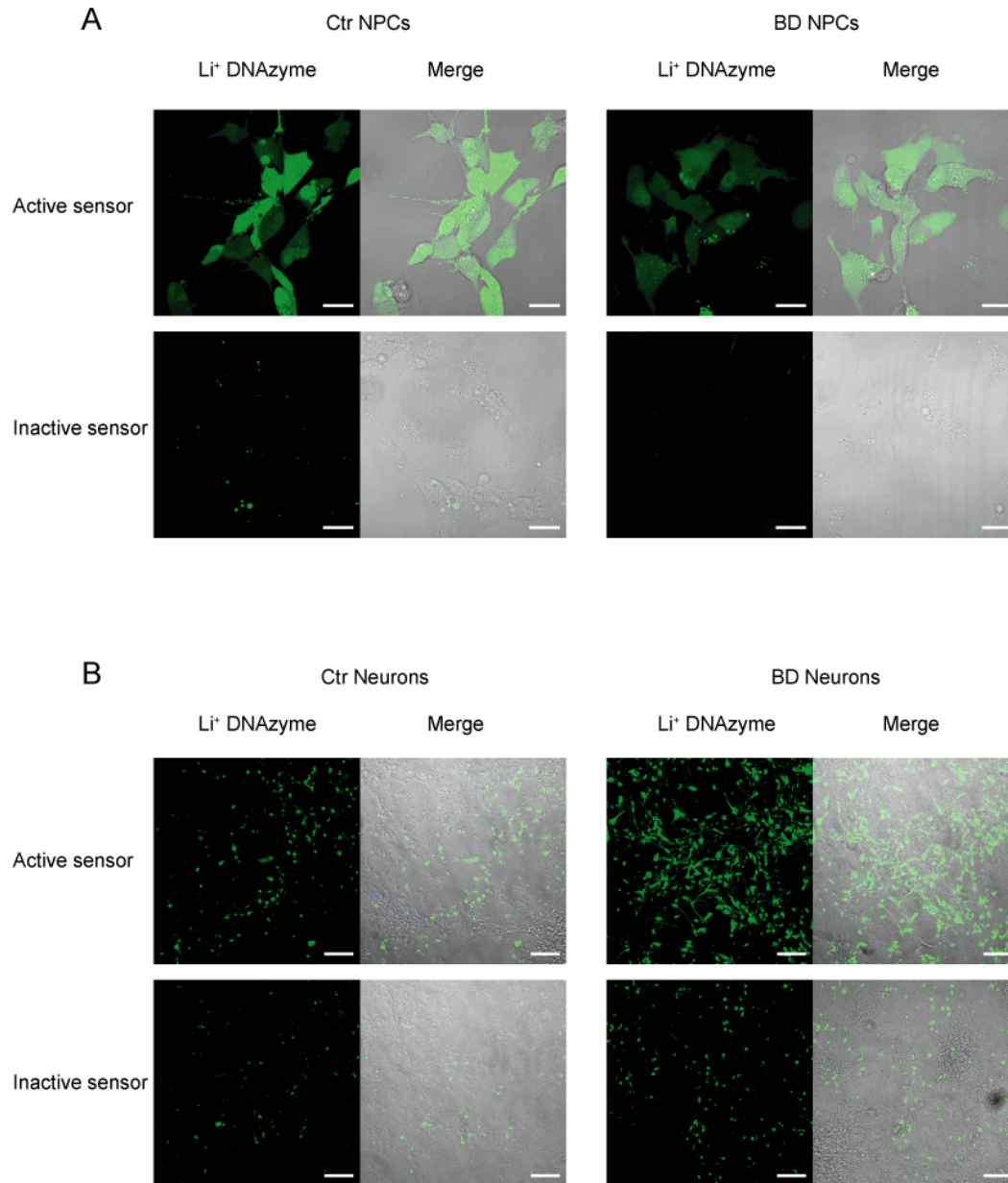


Figure S23. Intracellular Li<sup>+</sup> imaging in NPCs (A) and neurons (B) with active or inactive sensors after 3mM Li<sup>+</sup> treatment. Scale bar: 20  $\mu$ m (A); 100  $\mu$ m (B)

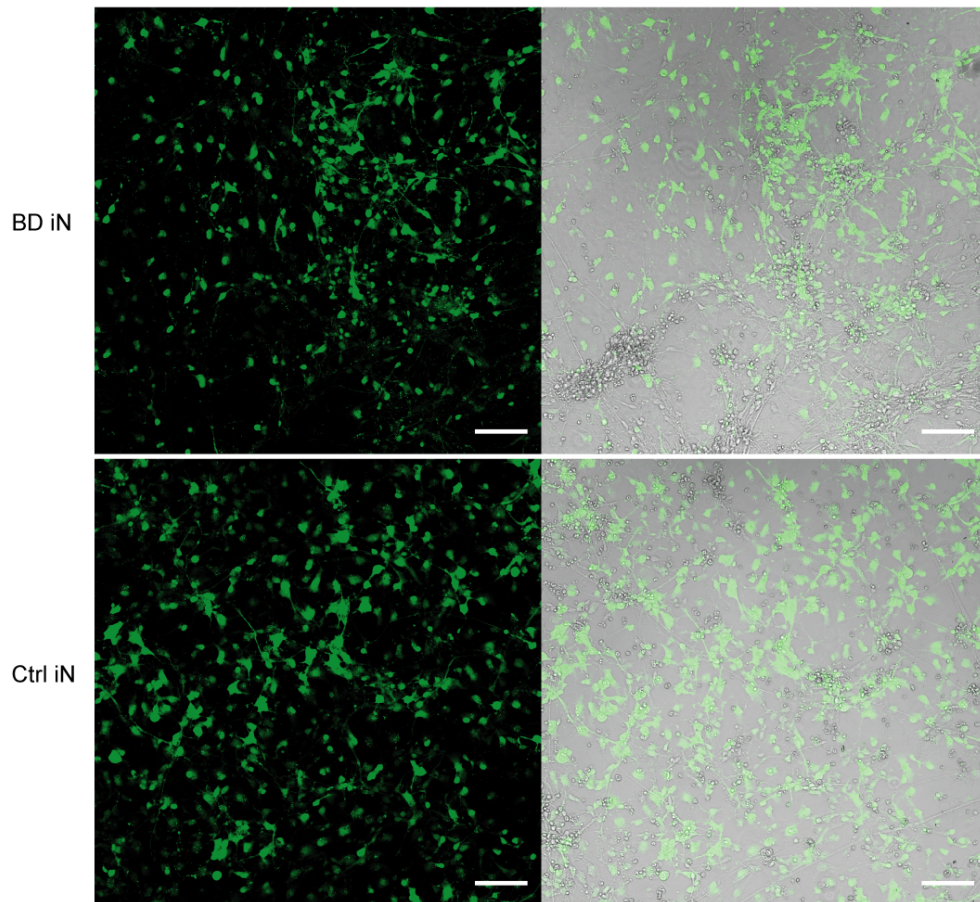


Figure S24. Positive transfection (control DNAzyme with fluorophores but without quenchers) in neurons with TurboFect. Scale bar: 100  $\mu$ m.



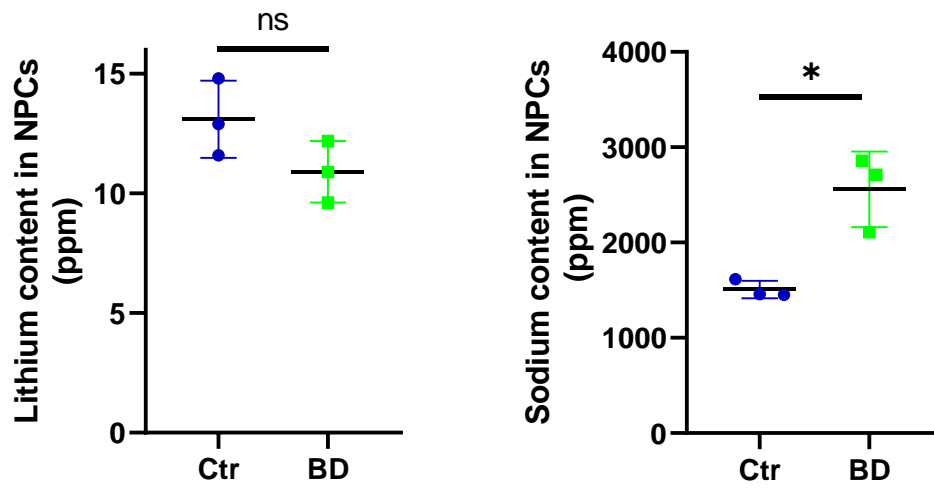


Figure S25. ICP detection of lithium (left) and sodium (right) total content in NPCs. ns  $p=0.139 > 0.05$ ; \*  $p=0.0112 < 0.05$  with two-tailed unpaired t test.